International Journal of Progressive Sciences and Technologies (IJPSAT)
ISSN: 2509-0119.

http://ijpsat.ijsht-journals.org
Vol. 19 No. 2 March 2020, pp. 48-64

# *Computational Study on Electronic Structure, Atomic Charges Distribution and Frontier Molecular Orbitals of Butadiene: General Features for Diels-Alder Reaction*

Anant Babu Marahatta[1, 2]

[1]Department of Chemistry, Amrit Science Campus, Tribhuvan University, Kathmandu, Nepal
[2]Chemistry Subject Committee, Kathford International College of Engineering and Management (Affiliated to Tribhuvan University), Kathmandu, Nepal



**Abstract – The electronic structure, Mulliken atomic charges distribution, and frontier molecular orbitals of the industrially important 1, 3-butadiene are investigated using computationally cheap yet decent first principles density functional theory (DFT) method. The DFT calculations confirm the planar molecular shape of the butadiene with two pairs of double bonds facing opposite directions of a sigma covalent bond where the steric effects from the two methylene groups are also significantly minimized. The inhomogeneous partial atomic charges distribution in the terminal and nonterminal carbon atoms approximated by the Mulliken population analysis method validates the existence of conjugated pi-bond regions in the butadiene system. Such bridging regions of the interjacent single bond are also reconfirmed by the DFT derived electron density surface maps of the HOMO and LUMO, where former orbital is localized mostly across the double bonded regions and the latter is across the single bonded regions; further reassures the pi-bonded regions of the butadiene as chemically more active sites. Again, the DFT predicted features of the butadiene-HOMO/LUMO as asymmetric/symmetric with single/double node/s respectively ascertains that the butadiene molecule stereochemically favors Diels-Alder chemical reactions while reacting with suitable dienophiles. This insight not only underscores the importance of electron density surface maps of the frontier molecular orbitals, their occupancy, symmetries, and stereoisomerism to Diels-Alder reactions but also strengthens computing ability of the DFT model.**

**Keywords – Butadiene, HOMO/LUMO, Mulliken Charges, Electron Density Surface Maps, Diels-Alder Reaction.**

## I. INTRODUCTION

In order to probe the most stable electronic structure (ground state structure) experimentally, the X−ray photoelectron spectroscopy (XPS), and X−ray emission spectroscopy (XES) are most commonly used instrumentation techniques [1]. Unlike in experimental research, a series of computing process has to be performed on the molecular specimen in theoretical/computational research while deriving several significant physicochemical properties. This process involves a quite advanced computational procedure that initially calculates the wave function and energy at a starting molecular geometry and then tests various possibilities to see which atomic arrangements and the electrons around the atom will give the lowest energy value [2]. Such repeated mathematical calculations usually generate the atomic coordinates of the most stable electronic structure of the molecule, dimensions of the optimized parameters such as atomic distances and angles, information about the frontier molecular orbitals (hereafter, FMOs) and their electron density surfaces, Mulliken atomic charges distribution, and electric dipole moments [3] [4]. In this contribution, a widely used tool of computational chemistry: Density Functional Theory (hereafter, DFT) model is employed to implement such powerful computing techniques and derived all of the mentioned characteristic features. Even

**Corresponding Author:** Anant Babu Marahatta

though this quantum mechanical model involves a mathematical formalism for approximately solving Schrodinger's wave equation, it produces better results than *ab initio* electronic structure methods at the similar computational cost [5], [6] and offers very promising practical computational electronic structure calculations across many disciplines of science. To the greatest extent, it is equally capable for treating weak noncovalent type interactions such as $\pi$-effects or $\pi$-interactions associating with conjugated $\pi$-bonding systems **[7], [8], [9].** This fact is also boosted by the previously reported DFT analyses on the effect of delocalized π-electron systems across the totality of the *n*-doped and undoped graphene surface of the same author [10], [11]. The author observed that all of the DFT derived characteristic features such as band-gap, Mulliken charges distribution, electronic structures etc. for both π-electron graphene systems are consistent with the experimentally produced results.

**In chemistry and material science,** a delocalization of π electron across the region of overlapping *p*-orbitals and its influence ($\pi$-effects or $\pi$-interactions) on the structural parameters is quite predominating more especially in the conjugated double bonded molecular systems. The 1,3-butadiene or simply butadiene is the simplest example of such system possessing conjugated π electrons as its IUPAC name and line-bond structure $CH_2$=CH−CH=$CH_2$ tells: 'buta' part is from butane, meaning 4 carbons; and the 'diene' means presence of two double bonded carbons or conjugated π-electrons. It is a colorless, non-corrosive gas having high volatility and low-water solubility, and is usually released into the environment through the industrial (butadiene production industry) and nonindustrial processes (automobile exhaust, cigarette smoke, and other combustion sources). It shows conformational isomerism: s-*trans* (both double bonds are on the opposite side of the sigma bond) and s-*cis* (both double bonds are on the same side of the sigma bond) conformers, that are interconvertible to each other at room temperature due to free unrestricted rotation about a sigma bond, as shown in Figure 1.The former conformer with a two-fold rotational axis $C_2$ is reported as energetically more stable than the latter conformer [12]. This is why, an isolated *s-trans* conformer is selectively chosen in this study as a molecular specimen for the DFT analysis on its electronic structure and stability, Mulliken charge distribution, and FMOs.

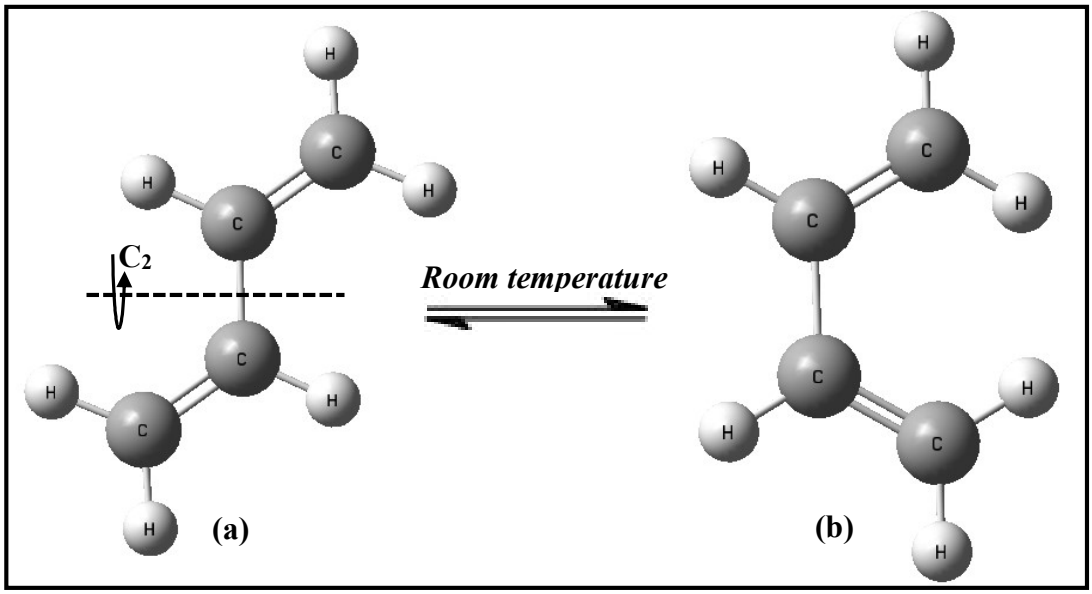


Figure 1. The structural interconversion of (a) *s-trans* and (b) *s-cis* butadiene conformers.

Industrially, butadiene is very important as a chemical intermediate and as a monomer in the production of polymers such as synthetic rubbers or elastomers [12] [13]. Even though, it is a versatile raw material used mostly in the production of styrene butadiene rubber (used in the manufacture of automobile tires), polybutadiene rubber (used as a high impact polystyrene), acrylonitrile-butadiene-styrene (used as thermoplastic resin in computers, radios, televisions etc.), nitrile rubbers (used in automobile industry) etc. [14], it's high global demand industrially is mainly due to its tremendous uses worldwide as tire raw materials and chemically is being a primary reagent in many organic

synthetic reactions such as Diels-Alder type organic reactions [15], [16], [17]. While this reaction brings following two components together *via* a cyclic transition state: "diene" comprising of two conjugated $\pi$-bonds and "dienophile" (diene-loving species) with at least one π-bond, the 1, 3-butadiene due to possessing **two** conjugated π-electron systems can readily undergo such reaction with both substituted or non-substituted ehene/ethyne systems [17]. When this reaction takes place, the former molecule behaves as a nucleophile (electron-rich species) and the latter as an electrophile (electron-poor species) resulting the shifting of four pi electrons of the diene and two pi electrons of the dienophile with the conversion of 2 π-bonds into 2 new stronger σ-bonds [18]. The chemistry of such typical chemical reaction involving pi electron systems as reactants can be more practically described by outer-edge orbitals interactions on the frontier of the molecule (frontier orbital interactions) [19]. In butadiene, such frontier molecular orbitals are produced as a result of superposition of the atomic orbitals. They tend to be the most spatially delocalized and have the highest and lowest energies, depending upon whether they are occupied or unoccupied by the electrons. The former type FMOs are known as “highest occupied molecular orbital” (hereafter, HOMO) and the latter type are “lowest unoccupied molecular orbital” (hereafter, LUMO) [19]. For the bond formation to take place in stereochemically favored Diels-Alder reaction, HOMO electrons of the diene (such as butadiene) must flow into the LUMO of the dienophile (such as ethene/ethyne). In this context, deriving a clear computational image of the electron density surfaces for the FMOs, partial atomic charges distribution, and thorough theoretical analyses of the butadiene HOMO, HOMO−1, LUMO, and LUMO+1 orbitals are very crucial as they are very essential while extracting the general features required to proceed butadiene involved Diels−Alder reactions.

Even though, several past intensive theoretical and experimental researches on the diene systems [15], [16], [17], [20], [21] have created many opportunities to encounter with previously under-researched or over-looked conjugated pi electron systems, the frequently released research reports and the repeated use of the butadiene in Diels-Alder reactions have still made butadiene a hot topic in synthetic organic/industrial chemistry and material science. More specifically, comparatively better theoretical/computational methodologies that can be used to compute the FMOs and their charge density contours, accessibility for occurring chemical reactions, specific localized sites, eigenvalues ($E$) and band gap ($\Delta E$), and electronic occupancy in the ground state as well as to determine the ground state electronic structure and Mulliken charges distribution in the butadiene are being widely sought. At present, the detailed DFT analyses on these specific features of the butadiene and their consequences to butadiene involved Diels-Alder reactions are reported. This research paper is organized as: Computational methods in section 2, Result and discussion in section 3, and Conclusion in section 4.

## II. Computational Methods

A trial structure of the *s-trans* butadiene with 4 carbon atoms and 6 hydrogen atoms in three dimensional (hereafter, 3D) axis was built by using GaussView visualization application software [22] as shown in chart 1. All the structural parameters of this initial structure are listed in fourth column of Table 1. The initial atomic Cartesian coordinates were extracted and used them to prepare *Gaussian* input file for computing ground state electronic structure. All the *Gaussian* keywords and methodologies were selected as instructed in *Gaussian* 09 manual [3]. The hybrid functional based DFT method known as B3LYP was used with the basis set of this type: 6−31G (d, p) i.e. the methodology used was DFT: B3LYP/6−31G (d, p). The better and more reliable computational results were assured by using the greater basis set of the type 6−31G (d, p) where the "6−31G" is the standard, split-valence double-zeta basis set, the functions that were used in *Gaussian* script computationally while describing the core and valence orbitals of the atoms; and the functions in parentheses "(d, p)" are polarization functions on heavy atoms and hydrogen that was used to properly describe chemical bonds [23]. Again, to make *Gaussian* for running desirable computation, the molecular charge and spin multiplicity was specified as two integers accordingly. Here, butadiene is a neutral species (charge = 0), and it is a spin-Singlet, with S = 0 and the multiplicity (2S + 1) = 1. Thus, the set of integer used to describe the neutral butadiene system was (0, 1). Moreover, while solving the electronic Schrodinger equation iteratively, the self-consistent field (hereafter, SCF) with both default SCF procedure (SCF=Tight) and Berny algorithm for optimizations to a local minimum were selected in *Gaussian* 09 [3] [24]. The *Gaussian* output files such as log, checkpoint (*.chk*), and formatted checkpoint (*.fchk*) files were read by using the *Gaussian* graphical interface i.e. GaussView [22] and various chemical data displayed in three dimensions were extracted. And then the optimized electronic structures, structural parameters such as bond lengths, bond angles, and torsional angles, Mulliken population analysis, electrons

distribution in the molecular orbitals, the 3D image for the HOMO, HOMO−1, LUMO, and LUMO+1 orbitals, the surface contour maps for the frontier molecular orbitals etc. of the butadiene were analyzed thoroughly.

**Chart 1.** The trial structure of *s-trans* butadiene. The brown and ash-brown colored spheroids represent C and H atoms respectively.

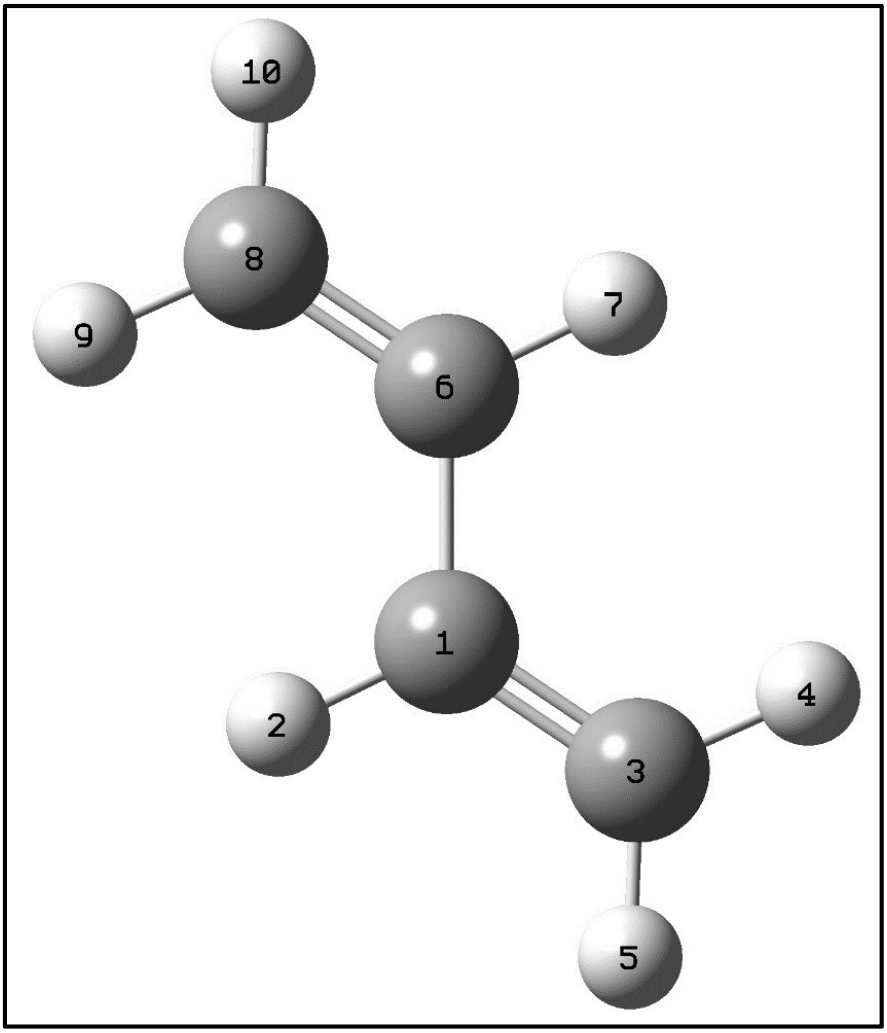


## III. RESULTS AND DISCUSSION

### 3.1 Ground state electronic structure

The DFT optimized geometry (no imaginary frequencies) of the s-trans butadiene visualized by Gaussview is shown in Figure 2 where brown and ash-brown spheroids represent C and H atoms respectively. For describing the optimized geometry more clearly, all the atoms present in the butadiene structure are labeled as C1, H2, C3, etc. While observing the optimized structure carefully, one can confirm the s-trans type conformation of the butadiene in which the molecule seems planar with the two pairs of double bonds facing opposite directions of an σ type single covalent bond. The structural stability of this conformer is also clearly seen as the steric effects from the two methylene (−CH2) groups are very much minimized and the H7 and H2 atoms are on the opposite side of the C6−C1 σ-bond. This leads to the very minimal or almost null magnitude of Van der Waals repulsion between H7 and H2 unlike in s-cis conformer (Figure 1) where these hydrogen atoms come “inside” while rotating C1−C6 σ-bond through a two-fold rotational axis C2 and hence, become in close proximity to each other. Moreover, the perfectly planar structure of the s-trans butadiene also allows for the maximum overlap between *p*-orbitals across the bonding

chain, creating conjugation across the whole molecule that ultimately stabilizes the molecule strongly. The same is the reason why many of the organic text books mention that maximum proportion of the butadiene (~ 96%) exists in the s-*trans* conformation at any one time.

Table 1: Comparison of the structural data for *s-trans* butadiene molecule

| Bond Lengths (nm), Bond Angles (°), Dihedral angles (°) | Experimental Methods | | *HF* calc [c] | Present work | |
|---|---|---|---|---|---|
| | Electron Diffraction [a] | Microwave [b] | | Trial structure | *DFT* calc *B3LYP/6-31G(d, p)* |
| C8=C6<br>C1=C3 | 0.1348 | 0.1337 | 0.1322 | 0.1320 | 0.1339 |
| C6−C1 | 0.1468 | 0.1467 | 0.1467 | 0.1467 | 0.1457 |
| C8−H10<br>C3−H5 | 0.1107 | 0.1085 | 0.1077 | 0.1072 | 0.1085 |
| C8−H9<br>C3−H4 | 0.1107 | 0.1087 | 0.1075 | 0.1074 | 0.1087 |
| C6−H7<br>C1−H2 | 0.1107 | 0.1089 | 0.1079 | 0.1076 | 0.1089 |
| H9−C8−H10<br>H5−C3−H4 | – | – | – | 116.411 | 116.723 |
| H10−C8=C6<br>H9−C8=C6<br>H4−C3=C1<br>H5−C3=C1 | 120.7 | – | 121.5 | 123.97 | 121.809<br>121.467<br>121.467<br>121.809 |
| H7−C6−C1<br>H2−C1−C6 | – | – | – | 116.123 | 116.271 |
| C8=C6−C1<br>C6−C1=C3 | 124.3 | 123.5 | 124.0 | 123.97 | 124.299 |
| H7−C6=C8<br>H2−C1=C3 | 120.7 | – | 121.5 | 119.905 | 119.428 |
| C8=C6−C1=C3 | – | – | – | 180.00 | 180.00 |
| H10−C8=C6−H7<br>H4−C3=C1−C6 | – | – | – | 0.00 | 0.00 |
| H10−C8=C6−C1<br>H5−C3=C1−C6 | – | – | – | 180.00 | 180.00 |

[a] See Reference 25; [b] Reference 26; and [c] Reference 27.

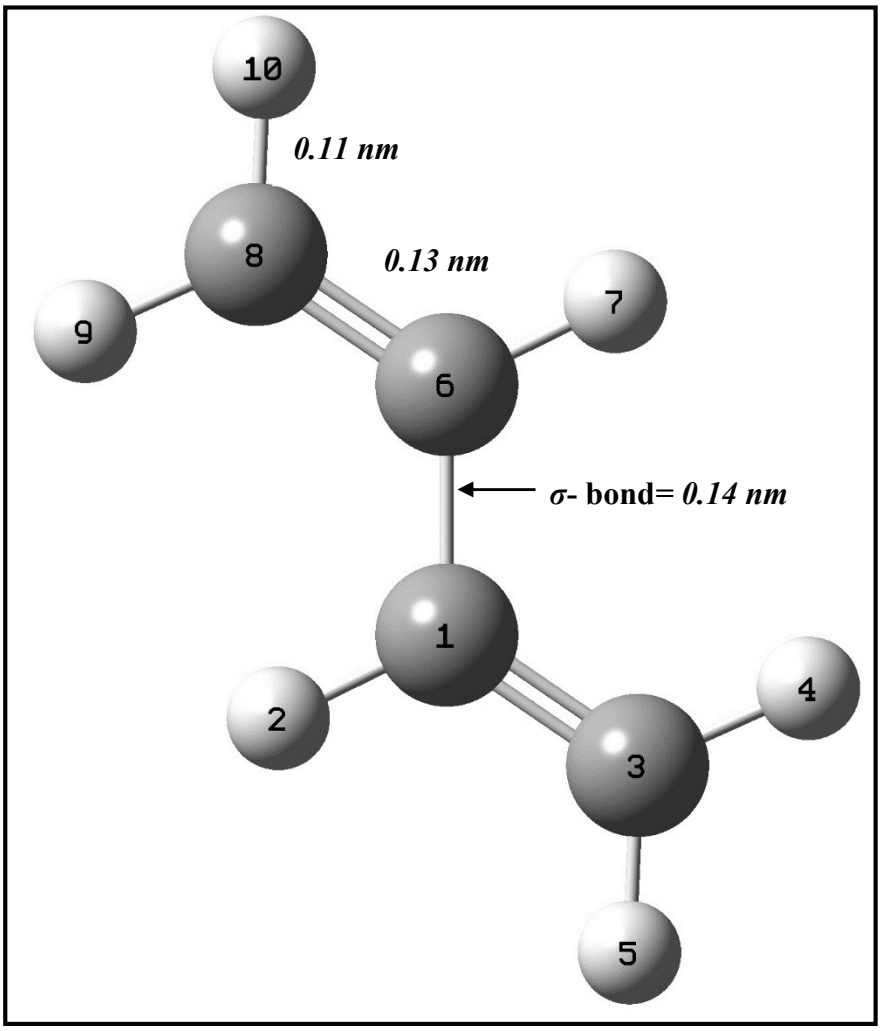


Figure 2. DFT optimized geometry of *s-trans* butadiene. The brown and ash-brown spheroids represent carbon and hydrogen atoms respectively.

As the optimized geometry is specified mostly in terms of the three parameters namely bond length: an average distance between the nuclei of two atoms bonded together in any given molecule; bond angle: angle formed between three atoms across the two bonds; and torsional angle: angle between the plane formed by the first three atoms and the plane formed by the last three atoms, the explicitly measured theoretically calculated values of them are listed in Table 1 where they are compared with the corresponding available values derived from the sophisticated instrumental tools (electron diffraction and microwave spectroscopy) and an ab initio Hartree-Fock (hereafter, HF) theoretical method. It is noteworthy here that all the DFT predicted structural data (bond lengths and bond angles listed in the 4th column of Table 1) are quite consistent with the experimentally derived (2nd column) as well as HF derived data (3rd column). Even though the dihedral angular values derived by the electron diffraction and microwave spectroscopy were unable to find out, the DFT predicted values are quite obvious and acceptable while realizing the planar structure of the s-trans butadiene as two faces of the type C8=C6 and C1=C3 are parallel as in tiling (dihedral angle = 180°) and two faces of the type H10−C8 and C6−H7 have antiparallel normal vectors (dihedral angle = 0°). This result is equally applicable to validate the real definition of S-trans confirmation given in organic chemistry text books: it is the confirmation of a single

σ-type covalent bond separating two double bonds in which the double bonds have a dihedral angle of 180°. More interestingly, the C=C and C−C bond lengths of the butadiene (double double-bonded compound) are found to be slightly shorter than in ethylene CH2=CH2 (single double-bonded compound: C=C bond length = 0.13305 nm) and ethane CH3−CH3 (electron-localized single bonded system: C−C bond length = 0.154 nm) respectively. This is due to the pronounced effect of π-electron delocalization that occurs more intensely in double double-bonded (two π bonds) system than in single double-bonded (single π-bond) system as observed by Craig et al. [28]. The intermediate C=C and C−C bond lengths indicate that each C−C bond in butadiene has partial double bond character, means the two sets of π electrons are not associated with any single atom or single covalent bond but are likely to be found equally anywhere along the carbon-carbon chemical bonds as in other conjugated π electron systems. Such resonating behavior of electrons is most commonly called electrons delocalization leading to extra stable molecule as a result of extending mobile electrons over the whole molecule. On the basis of two-center theory of valence bond theory (hereafter, VBT), such delocalization that results from the molecular stabilization is attributed to resonance. The same type of structural consequences caused by the π-electrons delocalization in butadiene were also elucidated by second order Møller −Plesset (MP2) perturbation theory elsewhere [28]. Furthermore, the variation in the bond angles from the original tetrahedral geometry of the carbon compounds can be described by the line-bond structure of the 1, 3-butadiene, CH2=CH−CH=CH2 where a double bond is in between C1 and C2, a single bond is in between C2 and C3, and another double bond is in between C3 and C4 (the atom numbering is in accordance with IUPAC rule). The terminal carbons C1 and C4 are attached to two H atoms while the central carbons C2 and C3 are attached to an H atom each. The formation of such bonding patterns can only be explained if all the four carbon atoms are in sp2 hybridized state, as postulated in the VBT of hybridization. The terminal carbons C1 and C4 use the three sp2 hybrid orbitals to form three sigma bonds, two with two H atoms and one with adjacent C atom while the central carbons C2 and C3 use their three sp2 hybrid orbitals to form one σ-bond with one H atom each and two with adjacent C atoms. According to the VBT, this type of hybridization involved in the orbitals on each carbon suggests that each bond angle must be in the range of 120° with trigonal planar geometry. This type of geometry can also be confirmed by the valence shell electron pair repulsion (VSEPR) theory as each C atom of the butadiene is directly bonded with three other atoms on the same plane. The slight deviation in the bond angles of these 2 sets, set 1: H7−C6−C1 and H2−C1−C6; set 2: H5−C3−H4 and H10−C8−H9 might be due to the effect of conjugated π-electrons that undergo resonance across the molecule.

### 3.2 Mulliken population analysis

A Mulliken population analysis [29] is the cheapest but fastest way to compute Mulliken atomic charges theoretically even though it tends to produce qualitative results at best. Such atomic charges can be used to characterize the electronic charge distribution in a molecule. More specifically, they are very useful to estimate the partial atomic charges qualitatively. For explaining the atomic charges distribution in a simple and understandable way, all the atoms of the butadiene are labeled as 1, 2, 3 etc. in accordance with the DFT computed electronic structure shown in Figure 2. The DFT computed charge distribution in the carbon and hydrogen atoms of the butadiene can be observed directly by the color of the spheroids in Figure 3 (color index and range are given in inset), where the most red colored (C3 and C8), and the most green colored (H5 and H10) spheroids represent the most negatively and the most positively charged carbon and hydrogen atoms respectively; the second most green colored (H9, and H4) and the least green colored (H7, and H2) spheroids represent the second most and the least positively charged hydrogen atoms respectively; the black−purple colored (C1, and C6) spheroids represent the negligibly least negatively charged or almost neutral atoms (neglecting −0.0 range) respectively. The Mulliken atomic charges in numerals are listed in Table 2, where the assigned atom numbers are in accordance with Figure 2 and Figure 3. By carefully analyzing such charge distributions, one can find that partial atomic charges of the terminal carbon atoms (C3 and C8) that are bonded to C atoms at one side by the double bonds ($1\sigma$ and $1\pi$ bonds) differ in wide range from those of the non−terminal carbon atoms (C1 and C6) that are bonded to each other by single covalent bond ($1\sigma$ bond). As the IUPAC name suggests, 1, 3−butadiene is composed of four C atoms with two adjoining conjugated $\pi$-bonds, the alternative distribution of $\pi$-electrons in the molecule may cause to distribute electrons inhomogeneously to the terminal and nonterminal carbon atoms resulting them the most and least negatively charged respectively. This acute negative charge distribution in the terminal carbon atoms of the butadiene reflect that these atoms act as the most probable reacting sites during the reaction with dienophiles (alkene/alkyne) in Diels-Alder type organic reactions in which the three double bonds in the two starting materials are converted into two new single

bonds and one new double bond. The same charge inhomogeneity among the carbon atoms ultimately makes nonuniform charge distribution in the attached hydrogen atoms: the most negatively charged carbon atoms hold the most positively charged hydrogen atoms and the least negatively charged carbon atoms hold the least positively charged hydrogen atoms. The charge inhomogeneity between carbon and hydrogen atoms is also governed by their respective electronegativity values $\chi$ ($\chi_C$ = 2.5 and $\chi_H$ = 2.1 in Pauling scale) that measures of an atom's ability to attract the shared-paired electrons of a covalent bond to itself. Even though, the absolute magnitude of the atomic charges computed by the Mulliken populations analysis displays a high degree of sensitivity to the types of basis set used, the qualitative values of them that are produced by the DFT:B3LYP/6−31G(d, p) method were presented. In future studies, the natural bond orbital (NBO) analysis [30] can be performed for more accurate distribution of the atomic charges.

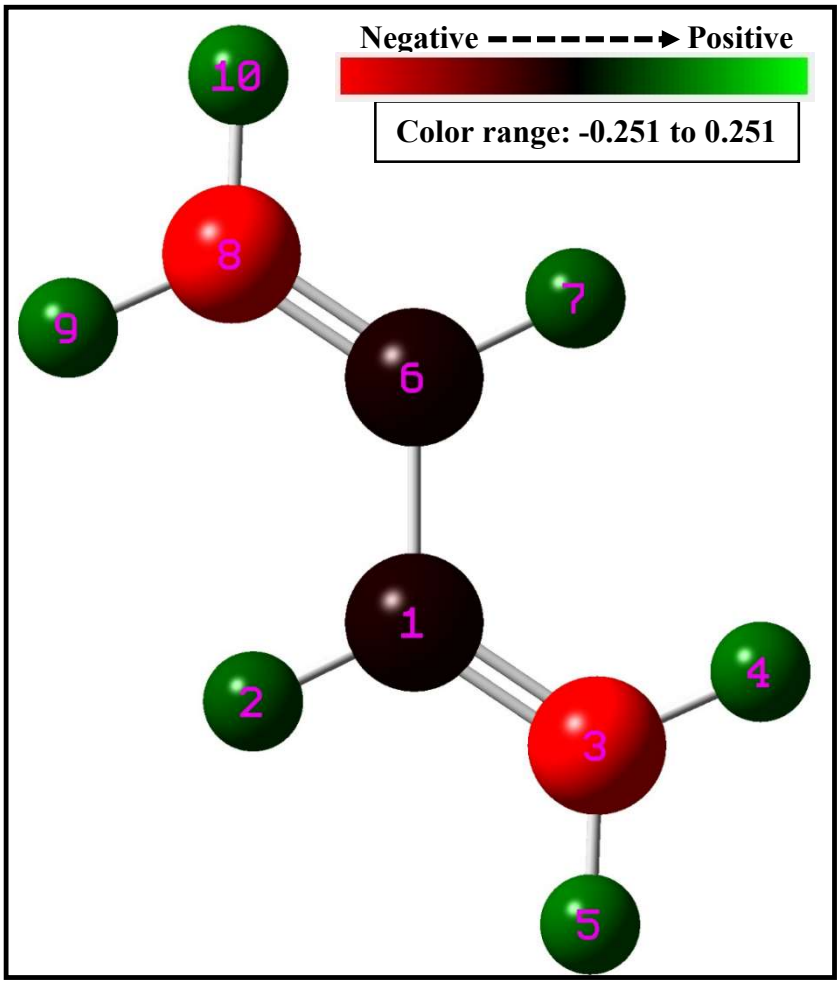


Figure 3. Mulliken charge distribution in DFT optimized geometry of butadiene. All the atoms are numbered as in Figure 2.

Table 2. Mulliken charge distribution in the carbon and hydrogen atoms of the butadiene [a]

| Atom label | Charge |
|---|---|
| C1 | -0.026 |
| H2 | 0.080 |
| C3 | -0.251 |

| | |
|---|---|
| H4 | 0.096 |
| H5 | 0.100 |
| C6 | -0.026 |
| H7 | 0.080 |
| C8 | -0.251 |
| H9 | 0.096 |
| H10 | 0.100 |

[a] all the atoms are labeled in accordance with the optimized geometry and Mulliken charge distribution shown in Figure 2 and Figure 3 respectively.

### 3.3 Frontier molecular orbitals

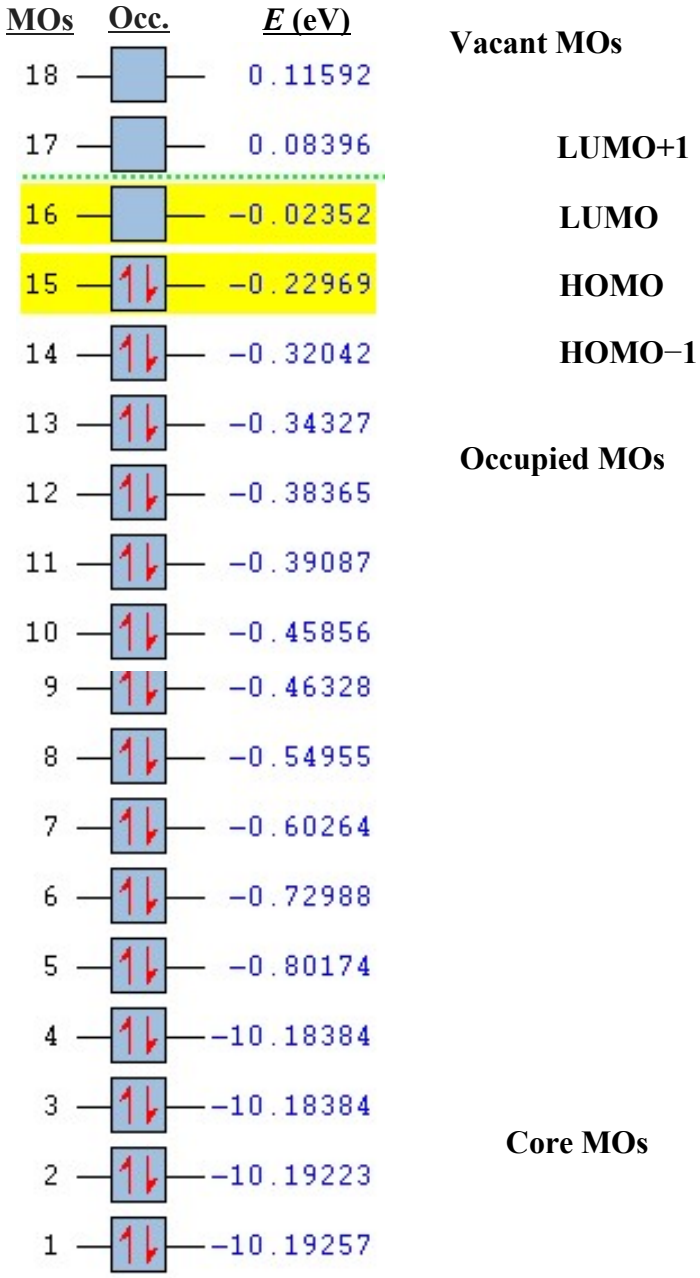


Figure 4. DFT computed electron orbital diagram of the butadiene. The first eighteen molecular orbitals (MOs) with their electron occupancy (Occ.) and eigenvalues (*E*) are shown. The HOMO and LUMO orbitals are highlighted.

According to the molecular orbital theory, the molecular orbitals (hereafter, MOs) are formed by the linear combination of the atomic orbitals (LCAO) or more specific, by the wave interaction of the atomic orbitals of two bonding atoms. In a butadiene molecule, twenty MOs (bonding and antibonding) are formed while combining twenty atomic orbitals associated with six hydrogen atoms and four $sp^2$ hybridized carbon atoms. As the electrons have one of two spins alpha ($ms = +1/2$) or beta ($ms = -1/2$), there are two lists of MOs, one for the alpha spin orbitals and another for the beta spin orbitals. Out of the several alpha type MOs (occupied and virtual), the first eighteen MOs with their occupancy (Occ.) and the respective eigenvalues in eV ($E$) are shown in Figure 4, where HOMO, HOMO−1, LUMO, and LUMO+1 are also marked. Among the MOs, the first fifteen are completely filled with electrons called occupied MOs and the remaining are vacant called unoccupied or virtual MOs. While scrolling to the bottom of this list of alpha orbitals (Figure 4), one can see the deepest core orbitals have almost identical energies, this means the alpha and beta electrons are in essentially the same spatial orbital and when the energy of the orbitals increases (while scrolling up), the difference in energy between the alpha and beta orbitals also increases resulting unequal energies among the outside orbitals. The energy level alignment of these orbitals indicates that the 15th MO is the highest energy orbital among the occupied MOs and the 16th MO is the lowest energy orbital among the unoccupied one. As the HOMO type molecular orbitals are low in energy than the LUMO type molecular orbitals, it is obvious for the electrons to be held in the former type orbitals by leaving the latter type orbitals vacant or unoccupied in the ground state. It can be seen in Figure 4 again that all the occupied MOs have a pair of electrons that usually have either alpha ($ms = +1/2$) or beta ($ms = -1/2$) spins, giving a net spin of 0 as all the alpha electrons cancel all of the beta electrons. Similarly, no any MOs are found to contain unpaired electron, indicating a total spin of 0 with a multiplicity of one or the singlet butadiene molecule. Such DFT predicted electronic distribution among the MOs suggests that the HOMO is an orbital of highest energy that is still occupied (in this case, 15th MO) and the LUMO is the lowest lying orbital that remains empty (in this case, 16th MO). Therefore, removing electrons from the HOMO and adding more electrons into the LUMO orbitals would be the easiest process energetically. It can further be explained by calculating energy gap between them. As the DFT computed eigenvalues for the HOMO and LUMO orbitals are of − 0.22969 eV and − 0.02353 eV respectively (Figure 4), the energy gap between them is calculated as: $\Delta E = [-0.02353 - (-0.22969)] = +0.20616$ eV. This energy gap tentatively speculates the first electronic transition energy of the butadiene. It can be interpreted in terms of an electronic transition between two energy levels, and hence the transition energy is the difference between the energies of the HOMO and LUMO levels.

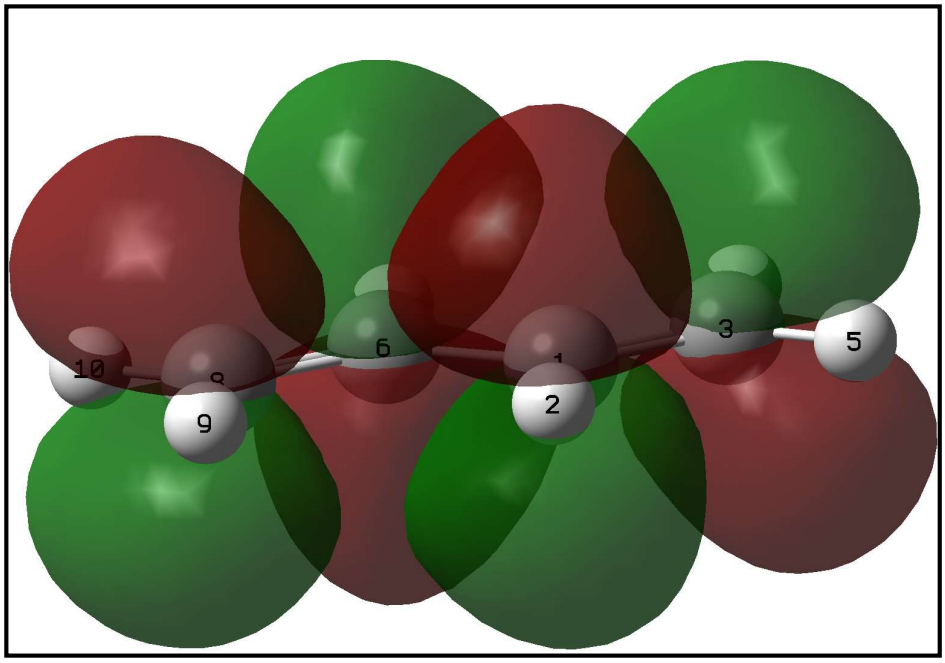


Figure 5. Four individual dumbbell shaped $p$ orbitals aligned with each other on the four carbon atoms: C3, C1, C6, and C8 of the butadiene.

The tendencies of undergoing electronic redistribution in those FMOs of the butadiene indicates that they can take part in the chemical reaction mechanisms (if they are of the correct symmetry: symmetry-allowed) that usually proceed by giving and/or taking electrons. Such type of reaction mechanisms involve creation or destruction of the covalent bonds through reduction, oxidation, and/or physisorption/chemisorption processes. For example, adsorption of the butadiene in Na−Y zeolite [31], on the Ag (110) [32] and Pd (110) [33] surfaces are such type reactions in which the FMOs show active participation. Katano *et al.* confirmed experimentally (by near edge X-ray absorption fine structure (NEXAFS) and scanning tunneling microscopy (STM)) that the 1, 3-butadiene is adsorbed on the Pd (110) surface through HOMO π-orbital [33]. Similarly, industrially important selective hydrogenation of the mono-π-adsorbed butadiene by Pd-activated $H_2$ [34] [35] is also a strong existing evidence of the HOMO orbital involvement in physisorption and chemisorption processes. Beside this, the energy of the HOMO and LUMO also gives an essential information about the behavior towards electrophilic reagents (or about the nucleophilic character of the molecule), and nucleophilic reagents (or about the electrophilic character of the molecule) respectively. As a rule, when the HOMO−LUMO gap is large, the nucleophilic and electrophilic characters are well marked. That is, the closer in energy between the HOMO (of nucleophile) and LUMO (of electrophile), greater will be an energy gain while proceeding chemical reactions, which ultimately makes reaction rate faster. Being the butadiene LUMO lower in energy (than ethene), it should be more reactive towards nucleophiles. In contrast to this, if the butadiene HOMO orbital doesn't present correct symmetry (symmetry-forbidden) during chemical reactions, the HOMO−1 orbital may show active involvement as its DFT computed eigenvalue is found to be quite close to that of the HOMO (Figure 4).

It is stated that the total number of molecular orbitals for a $\pi$-system is always equal to the number of the contributing *p* orbitals. As the name suggests, butadiene is composed of four carbons (C3, C1, C6 and C8) with four individual *p* orbitals aligned with each other as can be seen in Figure 5, the pi-systems of the butadiene must contain four π MOs including bonding and antibonding MOs. Among them, the C3=C1 and C6=C8 pi bonds of the butadiene have relatively high electron density as shown in Figure 6 by maroon colored mesh surfaces, and with the repulsive effect between the electrons, the energy of the HOMO pi orbital is high, meaning butadiene molecule behaves as a nucleophile. More precisely saying, the atomic sites where the pi bonds predominate act as proper attacking sites of the electrophiles. Additionally, while analyzing HOMO and LUMO surfaces shown in Figure 7, the most probable chemically active regions of the butadiene can be reconfirmed. Since, the HOMO orbital is found to be localized across the double bonded C3=C1 and C6=C8 regions while the LUMO orbital is localized across the single bonded C−C and C−H regions, and the HOMO electrons are the most available electrons to participate in a reaction, the pi bonded regions of the butadiene should be chemically more active. In particular, an image of the HOMO surface depicts that the frontier electron density is highest in the pi-bonding regions of C3, C1, C6, and C8, making these atoms the most probable chemically active sites. The same inhomogeneous chemical reactivity of the pi and sigma bonding regions of the butadiene was already observed by many experimental techniques while investigating the chemistry of the adsorbed and condensed butadiene molecules on the Na-Y zeolite [31], Ag (110) [32], and Pd (110) surfaces [33]. Hence, above presented DFT predicted results would be very much applicable to understand many significant and functional characteristics of the butadiene while behaving as an adsorbate on the substrate, accepting many electrophiles during Diels-Alder type reaction, synthesizing varieties of the organic compounds, carrying out industrially important selective hydrogenation reactions etc. These theoretically/computationally derived information would be ultimately utilized to route the reaction mechanisms of the butadiene involving organic chemical reactions that usually proceed through the series of the steps with many reaction intermediates or activated complexes.

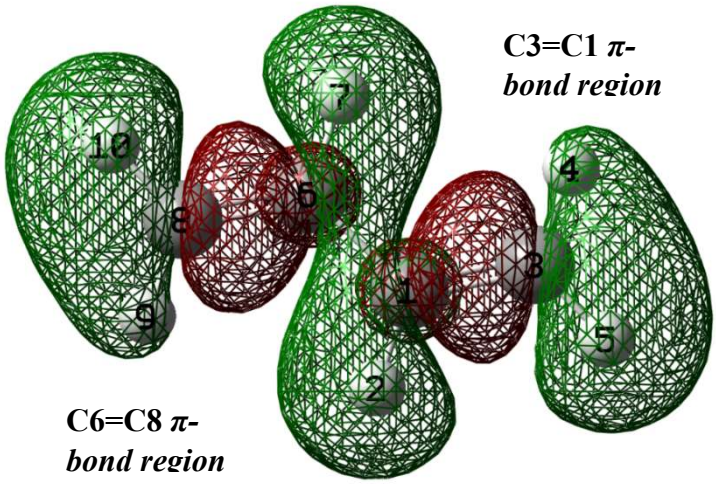


Figure 6. The maroon colored mesh surfaces (at an isosurface value = 0.02) across the π-bond regions (C3=C1 and C6=C8) of the butadiene represent localized electron density.

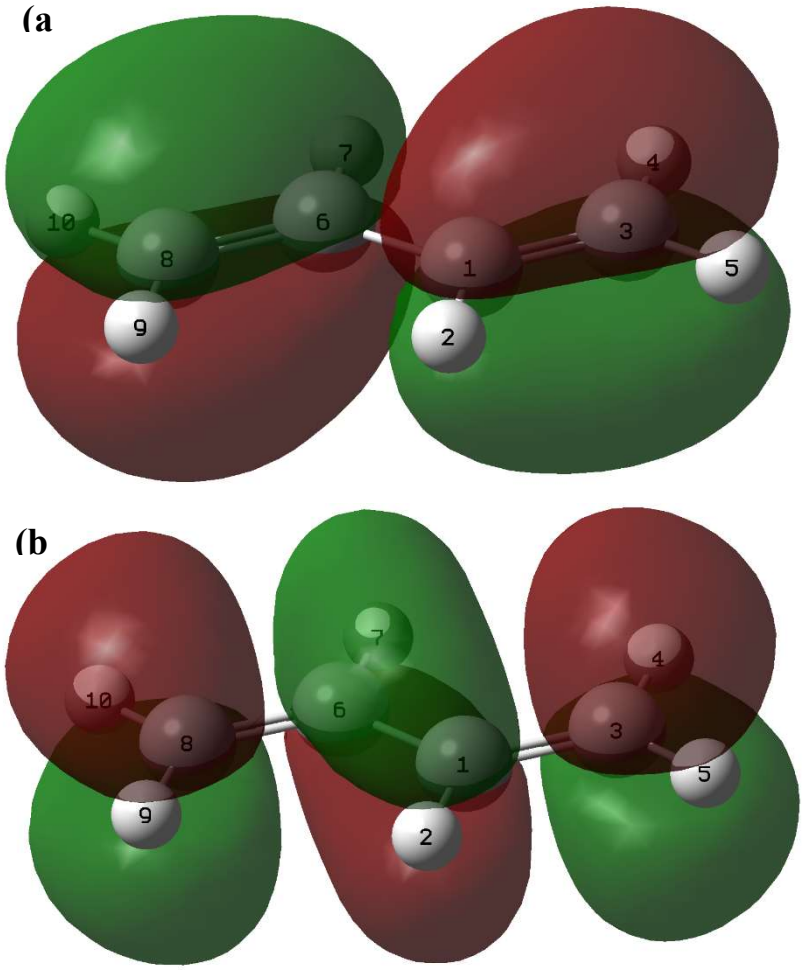


Figure 7. DFT derived (a) highest occupied molecular orbital (HOMO) and, (b) lowest unoccupied molecular orbital (LUMO) surfaces of the butadiene at an isosurface value of 0.02.

As can be derived from Figure 7(a), the highest occupied pi molecular orbital in the butadiene (i.e. HOMO) will have one node and be asymmetric (while converting into *s-cis* conformer), its electrons could flow to the antisymmetric LUMO of the dienophile easily while forming a new C−C sigma bond during Diels-Alder type organic reaction. Similarly, being butadiene LUMO orbital the lowest-energy unoccupied symmetric pi molecular orbital and will bear double nodes only after converting into the *s-cis* conformer (Figure 7(b)), its overlap with the symmetric HOMO of the another reacting species (such as dienophile) would be very favorable, suggesting that butadiene (or diene) molecule must adopt *s-cis* confirmation in order for the Diels-Alder type chemical reactions to occur. Again, unlike HOMO, the HOMO−1 has no nodes and is symmetric as can be seen in Figure 8(a), this feature of the orbital would remain unchanged but undergo rearrangement and become the HOMO of the Diels-Alder reaction product as explained elsewhere [36]. In the case of LUMO+1, there are four nodes and is asymmetric (Figure 8(b)), this feature would also remain unchanged while it rearranges to become the LUMO of the reaction product. An alternative description to support these features is that the butadiene molecule demonstrates stereoisomerism in the Diels-Alder reaction, and when it does, its relative configuration is preserved in the additive or Diels-Alder product. Even though the *s-cis* conformer of the butadiene is preferable for Diels-Alder type reaction, both the *s-cis* and *s-trans* conformers are generally in rapid equilibrium (Figure 1), permitting the use of both. Thus, the above descriptions of the DFT derived MOs occupancy and their symmetries would be highly applicable while interpreting Diels-Alder type reaction mechanisms in organic chemistry.

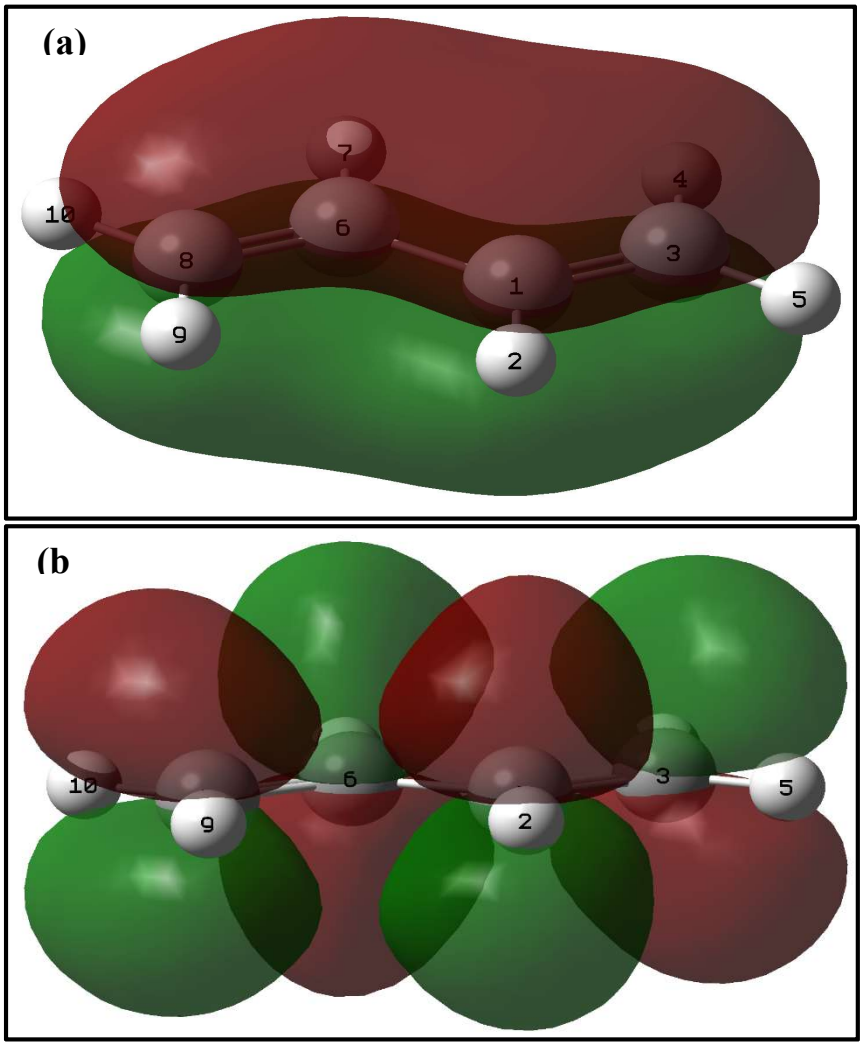


Figure 8. DFT derived (a) HOMO−1 and, (b) LUMO+1 surfaces of the butadiene at an isosurface value of 0.02.

In short, with these consequences of the HOMO−LUMO energy gap $\Delta E$ and their electron density surfaces in predicting nucleophilicity and chemically active sites of the butadiene, the ΔE not only approximates the band gap between the valence band and the conductance band of this molecule but also speculates its lowest energy transition frequency in UV visible spectroscopy. In principle, if the distribution of the energy throughout the molecule occurs, the HOMO−LUMO gap will be smaller that corresponds to better stability. It particularly happens in a conjugated π-orbital systems including in butadiene due to the mobility of the π-electrons [37]. Such electronic mobility further means that the butadiene must have a good ideal gas heat capacity and thermal conductivity as described *elsewhere [38]* and hence, it can be used to manufacture conductive ABS (Acrylonitrile Butadiene Styrene) filaments that works great for electronic enclosures, circuit boards, and various gadgetries requiring electrostatic protection [39].

As it is discussed in subsection 3.2, the carbon spheroids #3 and #8 are the most negatively charged carbon atoms predicted by the Mulliken population analysis method. Interestingly, the LUMO orbital is found to be localized in the same atoms (along with other atoms) unlike HOMO orbital. It can be clearly observed in Figure 7(b). Such electron density localization of the specific molecular orbital might be due to increasing in-phase type of electron waves interaction caused by the excessive accumulation of the negative charge on the C3 and C8 atoms. The molecular orbital resulting from such in-phase type of electron wave interaction would be bonding LUMO. This bound state of LUMO orbital is due to increase in attractions between electrons and nuclei that is again caused by the excessive negative charge accumulated on the C3 and C8 atoms. The same can be justified by the DFT predicted negative eigenvalues for LUMO (− 0.02352 eV) orbital (only the bonding orbitals have negative eigenvalues).

In order to examine the maximum concentration of the orbital charge density on the C−C, C=C and C−H bond axes of the butadiene, the transparent surfaces of the HOMO/LUMO molecular orbitals are produced from the DFT predicted data. For this, the charge density contours mode that allows one to display volumetric results in a plane is selected. Among them, the contours in a plane for the HOMO type MOs are shown in Figure 9, where one can find that the simple LCAO description has accounted the principal features of this molecular orbital. More concrete information that can be drawn from the contours map is: (i) the orbital charge density is found to be concentrated fully along each C−C, C=C, and C−H bond axes that draws the bonding-atoms nuclei together, which ultimately act as a binding force for the bonding atoms, and (ii) the orbital charge density is inhomogeneously distributed as can be seen more especially in between C and H atoms. Thus, being able to generate transparent surfaces of the orbitals, the charge density contour maps is very useful to reconfirm the planar and conjugated bonding patterns of the carbon and hydrogen atoms in the butadiene. Since, in the DFT−SCF method input, a basis set is used to represent the electronic wave function that is composed of atomic orbitals, but they never represent the actual dwelling of the electrons. However, after converging the DFT−SCF computational procedure for a given set of orbitals and coefficients, the well-defined shape of the orbital representing an actual charge density blob is produced. Including the orbital electron density surfaces, the DFT−SCF output also contains Cartesian coordinates of the molecule and orbital specifications including the number of occupied and virtual orbitals in each orbital symmetry. The iso-(electron) probability surfaces of the molecular orbital interpretation of the butadiene is shown in Figure 10, where they show the electron probability density of the atoms/molecules in space and also demonstrate well about the wave nature of the electrons: “no electrons reside in the orbitals”. Even though these calculated iso-probabilities should not be equated with the real images of the molecular orbitals, they can’t be considered separately either for the practical purposes.

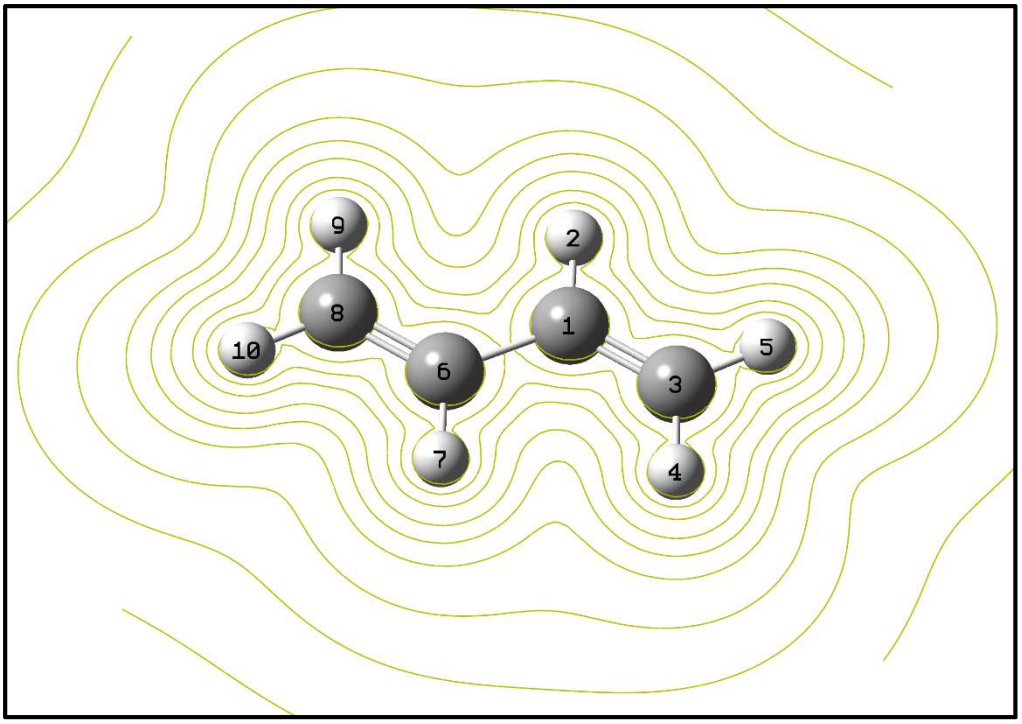


Figure 9. The charge density contours map for the HOMO type molecular orbital of the butadiene.

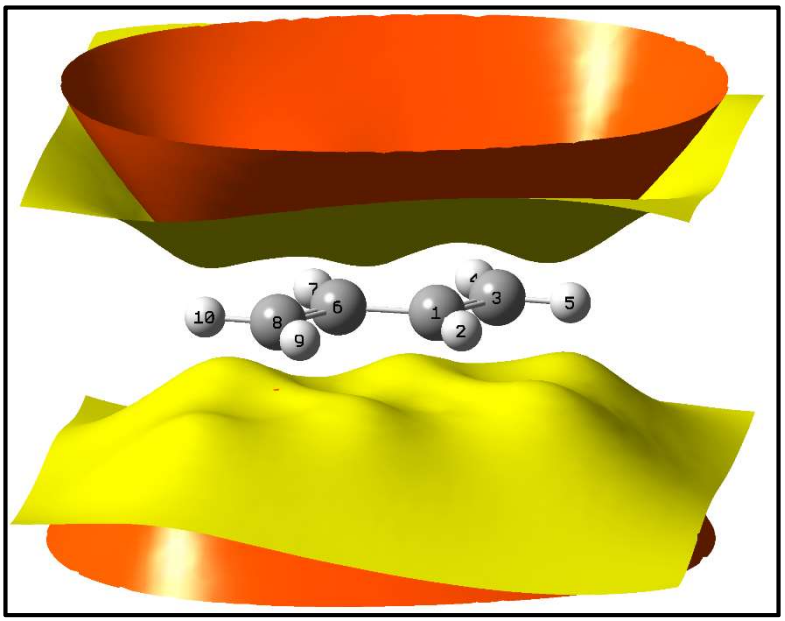


Figure 10. Iso-(electron) probability surfaces of the molecular orbital interpretation of the butadiene.

## IV. Conclusion

In this contribution, the theoretical results computed by the density functional theory (DFT) model are presented while applying it to the butadiene molecular specimen. As it provides a way to systematically map the many body problem onto a single-body problem, it presently unveiled an extensive knowledge for interpreting at least few unique characteristics of such diene system. At first, the energetically most stable electronic structure of the s-trans butadiene is produced by the DFT: B3LYP/6−31G (d, p) methodology, and then confirmed its planar molecular shape with two pairs of double bonds facing opposite directions of an σ type single covalent bond. In the same DFT derived ground state electronic structure, the steric effects from the two methylene (−CH2) groups are found to be very much minimized representing it as an extra stable structural conformer of the butadiene. The DFT computed dimensions of the structural parameters such as bond length, bond angle, and torsional angle of this low energy structure are found to be as equal as the experimentally and ab initio HF derived values. More interestingly, intermediate length of the C=C and C−C bonds measured in the same DFT optimized structure elucidated the existence of conjugate double bond character in each C−C bond of the butadiene. Along with this, the electronic charge distribution investigated qualitatively by the cheapest but fastest Mulliken population analysis method shows that the partial atomic charges of the terminal carbon atoms (C3 and C8) bonded at one side to the C atoms by the double bonds (1σ and 1π bonds) differ in wide range from those of the non-terminal carbon atoms (C1 and C6) bonded to each other by the single covalent bond (1σ bond). Similarly, the DFT computed electronic configuration in the different molecular orbitals of the butadiene clarified that HOMO is the orbital of highest energy ($E1 = -0.22969$ eV) that is still occupied and LUMO is the lowest lying orbital ($E2 = -0.02353$ eV) that remains empty. The energy gap between these two frontier molecular orbitals (FMOs) not only tentatively speculated the first electronic transition energy of the butadiene and marked its extreme reactivity towards electrophiles but also proved the HOMO/ LUMO tendencies of involving in the chemical reaction mechanisms. Furthermore, the electron density surface maps of the HOMO and LUMO orbitals depicted that former orbital has maximum localized sites across the double bonded (C3=C1 and C6=C8) regions while the latter orbital is localized across the single bonded (C−C and C−H) regions, and being the HOMO electrons most available to participate in the chemical reactions, the pi bonded regions of the butadiene are predicted as chemically more active regions. Again, the DFT predicted single node and asymmetric nature of the butadiene HOMO surface supports easy flow of electrons towards the antisymmetric LUMO of the dienophile, and double nodes and symmetric nature of the butadiene LUMO favors its overlap with the symmetric HOMO of the dienophile while developing a new C−C σ-bond in Diels−Alder type chemical reaction. In a similar way, many useful information related to orbital charge density concentration along each type C−C and C−H bond axis, and planar bonding patterns of the carbon and hydrogen atoms derived from the charge density contours in a plane for the HOMO type molecular orbitals reconfirmed the butadiene geometry in the 3D space.

The results achieved in this study even by using computationally cheap yet decent theoretical model will be very useful while tuning HOMO/LUMO properties of the diene systems. More specifically, the DFT derived HOMO/LUMO electron density surfaces, their occupancy, symmetries, and nodes of the diene systems would be highly applicable while interpreting Diels−Alder type reaction mechanisms in organic chemistry. It is believed that present theoretical contribution has not only produced a capacious knowledge for explaining at least few unique characteristics of the diene systems while reacting with dienophiles, but also strengthened the extraordinary skills that the DFT model possess in computing ground state electronic structures, Mulliken charge distribution, and frontier molecular orbitals for the substituted and nonsubstituted diene/dienophile systems. With this, the DFT−SCF methodology puts considerable demand on the accuracy of the computational/theoretical methods for investigating electronic properties of the multiple double-bonded conjugated pi electron systems.

## References

[1] Yu. Khyzhun, T. Strunskus, S. Cramm and Yu. M. Solonin, J. Alloys Compd. 389, 14 (2005).
[2] R. Daudel, Electronic Structure of Molecules (Elsevier, 1966).
[3] Gaussian 09 manual. http://gaussian.com/geom/?tabid=1#GeomkeywordReadOptimizeop tion
[4] M. J. Frisch, G. W. Trucks, H. B. Schlegel, G. E. Scuseria, M. A. Robb, J. R. Cheeseman, G. Scalmani, V. Barone, G. A. Petersson, H. Nakatsuji et al. Gaussian 09, Revision C.01 (Gaussian, Inc. 2004).
[5] P. Hohenberg and W. Kohn, Phys. Rev. B. 136, 864 (1964).
[6] Kohn and L. Sham, Phys. Rev. J. 140, A1133 (1965).

[7] G. A. Dilabio and A. Otero-de-la-Roza Ed. Abby L. Parrill, Kenny B. Lipkowitz ch. 1 (Reviews in Computational Chemistry, 2016).
[8] [C. Corminboeuf, Acc. Chem. Res. 47(11), 3217(2014).
[9] T. J. Mooibroek, Molecules 24, 3370 (2019).
[10] A.B. Marahatta, Int. J. Prog. Sc. Tech. 16 (2), 01(2019).
[11] B. Marahatta, Int. J. Prog. Sc. Tech. 16 (1), 51(2019).
[12] Butadiene Product Summary, American Chemical Council. https://www.americanchemistry.com/ProductsTechnology/Olefins/Butadiene-Product-Summarypdf.pdf
[13] N. C. Craig, P. Groner and D. C. McKean, J. Phys. Chem. A, 110(23), 7461(2006).
[14] ICIS, Butadiene Uses and Market Data (2010) https://www.icis.com/explore/resources /news/2007/11/01/9075172/butadiene-uses-and-market-data/
[15] Hunt, Conjugation in Alkadienes and Allylic Systems, ch. 10, Department of Chemistry, University of Calgary.
[16] K. C. Nicolaou, S. A. Snyder, T. Montagnon and G. Vassilikogiannakis, Angewandte Chemie: J. Ger. Chem. Soc. 41(10), 1668 (2002).
[17] E. J. Corey, Angewandte Chemie: J. Ger. Chem. Soc. 41(10), 1650 (2002).
[18] M. Wang, Z. H. Liu, Y. K. Chen, J. M. Han, Y. L. Chen, M. M. Miao and H. Cao, Comp. Th. Chem. 1017, 174 (2013).
[19] K. Fukui, T. Yonezawa and H. Shingu, J. Chem. Phys. 20 (4), 722(1952).
[20] V. Termath, D. J. Tozer and N. C. Handy, Chem. Phys. Lett. 228, 239(1994).
[21] Y. Hu and Y. Yu, Comp. Mat. Sci. 161, 321(2019).
[22] Æ. Frisch, H. P. Hratchian, R. D. Dennington II, T. A. Keith and J. Millam, Gauss view 5 Reference, (Gaussian, Inc. 2009).
[23] J. B. Foresman and Æ Frisch, Exploring Chemistry with Electronic Structure Methods, 3rd ed., Gaussian, Inc.: Wallingford, CT, 2015.
[24] Æ Frisch, Gaussian 09W Reference, Gaussian, Inc.: Wallingford, CT, 2009.
[25] K. Kveseth, R. Seip and D. Kohl, Acta Chem. Scand. A 34, 31(1980).
[26] W. Caminati, G. Grassi and A. Bauder, Chem. Phys. Lett. 148, 1988(13).
[27] W. Bock, P. George and M. Trachtman, Theor. Chim. Acta, 64, 1984(293).
[28] N. C. Craig, P. Groner and D. C. McKean, J. Phys. Chem. A, 110(23), 7461(2006).
[29] R.S. Mulliken, J. Chem. Phys. 23, 1833(1955).
[30] R. S. Mulliken and W. C. Ermler, Diatomic Molecules: Results of Ab Initio Calculations pp. 33-38, (Academic, New York, 1977).
[31] S. Gautam, S. Mitra, S. L. Chaplot and R. Mukhopadhyay, Phys. Rev. E, 77(6), 061201(2008).
[32] Coulman, J. L. Solomon, R. J. Madix and J. Stöhr, Surface Science 257(1), 97(1991).
[33] S. Katano, S. Ichihara, H. Ogasawara, H. Kato, T. Komeda, M. Kawai and K. Domen, Surface Science 502, 164(2002).
[34] N. Masoud, C. Calers and P.E.de Jongh, ChemCatChem 9(12), 2418(2017).
[35] Y. Feng, L. Zhou, Q. Wan, S. Lin and H. Guo, Chem. Sci. 9, 5890 (2018).
[36] Organic Chemistry Portal, Diels-Alder Reaction, https://www.organic-chemistr y.org/namedreactions/
[37] M. S. Dresselhaus, P. C. Eklund and G. Dresselhaus, Carb. Mat. Adv. Tech. 36, 35 (1999).
[38] Dortmund Data Bank, http://ddbonline.ddbst.com/DDBSearch/onlineddboverview.exe? submit=Details&systemcomplist=364
[39] Conductive ABS Filament – 1.75mm or 3mm http://www.3dprinterpro.com/pr/conductive -abs-filament/